

# Two-photon double ionization of helium in the region of photon energies 42-50 eV.

I. A. Ivanov<sup>\*†</sup> and A. S. Kheifets

*Research School of Physical Sciences and Engineering,  
The Australian National University, Canberra ACT 0200, Australia*

(Dated: February 9, 2008)

## Abstract

We report the total integrated cross-section (TICS) of two-photon double ionization of helium in the photon energy range from 42 to 50 eV. Our computational procedure relies on a numerical solution of the time-dependent Schrödinger equation on a square-integrable basis and subsequent projection of this solution on a set of final states describing two electrons in continuum. Close to the threshold, we reproduce results previously known from the literature. The region 47 – 50 eV seems to have been previously unexplored. Our results suggest that TICS, as a function of the photon energy, grows monotonously in the region 42 – 50 eV. We also present fully resolved triple differential cross sections for selected photon energies.

---

<sup>\*</sup> Corresponding author: Igor.Ivanov@anu.edu.au

<sup>†</sup> On leave from the Institute of Spectroscopy, Russian Academy of Sciences

## I. INTRODUCTION

Multi-photon atomic ionization resulting in ejection of a single electron, as well as other single active electron phenomena in intense laser fields, are relatively well understood by now [1]. In contrast, strong field ionization with several active electrons involved is a much more challenging problem in which the highly nonlinear field interaction is entangled with the few-body correlated dynamics [2]. The two-photon double-electron ionization (TPDI) of helium is the archetypal reaction of this kind. Even for this simplest many-photon many-electron process, non-perturbative treatment of the external field is essential as well as a proper account of correlation in the two-electron continuum. Neglect of either aspects of TPDI results in a gross failure. In Ref. [3], for instance, it was demonstrated that a perturbative treatment of the external field in this process can lead to an order of magnitude error in the cross-sections even for relatively mild fields.

Because of canonical importance of the TPDI of He, a number of theoretical methods have been developed and applied to this problem recently. Among them are the so-called many-electron many-photon theory [4, 5], the *R*-matrix Floquet approach [6], and various time-dependent approaches [3, 7, 8, 9, 10, 11, 12]. These studies allowed to achieve considerable progress in theoretical modelling of TDPI in helium. As far as total ionization cross section (TICS) is concerned, the region of the photon energies from the threshold (38.5 eV) to 47 eV is well understood. Various methods, such as the time-dependent close-coupling (TDCC) approach [3, 13, 14] and the *R*-matrix Floquet method [6], gave results which lie sufficiently close to each other, and which indicate that in this region of the photon energies TICS is a monotonously growing function of the energy. In Ref. [15] the presence of a maximum of TICS in the vicinity of 42 eV was reported. For larger energies, the authors found that TICS starts decaying monotonously. Overall shape of TICS, as a function of the photon energy, was found to be very similar to that of single-photon double ionization. However, this finding contradicts to other reports which indicated no maximum anywhere below 47 eV.

In the present work, we report the behavior of TICS of TPDI of helium at larger energies from 47 to 50 eV. This photon energy range seems to be unexplored up to now. Our results indicate that TICS continues to grow in this region of energies.

As a computational tool, we used a method which we proposed recently for single photon double ionization studies [16]. The method is based on a numerical integration of the time-dependent Schrödinger equation (TDSE) with subsequent projection of the solution on a set of the field-free final states of the helium atom with both electrons in continuum. Accurate description of these states is by itself a rather complicated problem. In Refs. [17, 18], inter-electron correlations in the final state was taken into account perturbatively. One can also address this problem using the exterior complex scaling method [19, 20, 21] or using the complex Sturmian basis [22]. The hyperspherical R-matrix method with semiclassical outgoing waves [23] and various implementations of the close-coupling method [14, 24, 25, 26] were also used.

In our earlier work [16], we proposed to use the so-called convergent close-coupling (CCC) expansion [27] to describe the field-free two-electron continuum in conjunction with solution of TDSE. In that paper we considered effect of the external DC electric field on the single-photon double-electron ionization cross section. In the present work, we apply this method for the study of two-photon double electron ionization of helium.

The paper is organized as follows. In the next section we give an outline of the theoretical procedure. Then we discuss the results we obtained for the integrated and fully differential cross sections of TPDI of helium.

## II. THEORY.

Detailed description of our method can be found in Ref. [16]. We shall present here only a brief description of the computational procedure. At the first step we solve numerically the TDSE for the helium atom in the presence of the external ac field:

$$i \partial \Psi / \partial t = \hat{H} \Psi, \quad (1)$$

where:

$$\hat{H} = \hat{H}_0 + \hat{V}_{12} + \hat{H}_{\text{int}}(t), \quad (2)$$

where the non-interacting Hamiltonian and the Coulomb interaction are, respectively,

$$\hat{H}_0 = \frac{\mathbf{p}_1^2}{2} + \frac{\mathbf{p}_2^2}{2} - \frac{2}{r_1} - \frac{2}{r_2}, \quad (3)$$

$$\hat{V}_{12} = \frac{1}{|\mathbf{r}_1 - \mathbf{r}_2|}. \quad (4)$$

The interaction with the external ac field is written in the length gauge:

$$\hat{H}_{\text{int}}(t) = f(t)(\mathbf{r}_1 + \mathbf{r}_2) \cdot \mathbf{F}_{\text{ac}} \cos \omega t \quad (5)$$

Here  $f(t)$  is a smooth switching function which is chosen in such a way that the amplitude of the field remains constant during the time interval  $(T, 4T)$ , where  $T = 2\pi/\omega$  is a period of the ac field. This field is ramped on and off smoothly over one ac field period. The total duration of the atom-field interaction is therefore  $T_1 = 6T$ .

The solution of the TDSE is sought in the form of expansion on a square-integrable basis

$$\Psi(\mathbf{r}_1, \mathbf{r}_2, t) = \sum_j a_j(t) f_j(\mathbf{r}_1, \mathbf{r}_2). \quad (6)$$

Here

$$f_j(\mathbf{r}_1, \mathbf{r}_2) = \phi_{n_1 l_1}^N(r_1) \phi_{n_2 l_2}^N(r_2) |l_1(1) l_2(2) L\rangle, \quad (7)$$

where notation  $|l_1(1) l_2(2) L\rangle$  is used for bipolar harmonics. The radial orbitals in Eq. (7) are the so-called pseudostates obtained by diagonalizing the  $\text{He}^+$  Hamiltonian in a Laguerre basis [25]:

$$\langle \phi_{nl}^N | \hat{H}_{\text{He}^+} | \phi_{n'l'}^N \rangle = E_i \delta_{nn'} \delta_{ll'} \quad (8)$$

In the present work, we consider electric field of the order of 0.1 a.u. corresponding to  $3.5 \times 10^{14} \text{ W/cm}^2$  intensity. For this, not very high intensity, we can retain in the expansion (6) only the terms with total angular momentum  $J = 0 - 2$ . To represent each total angular momentum block, we proceed as follows. For all  $S$ ,  $P$ ,  $D$  total angular momentum states we let  $l_1, l_2$  vary within the limits  $0 - 3$ . The total number of pseudostates participating in building the basis states was 20 for each  $l$ . To represent  $J = 0, 1, 2$  singlet states in expansion (6), we used all possible combinations of these pseudostates. Such a choice gave us 840 basis states of  $S$ -symmetry, 1200 basis states of  $P$ -symmetry and 1430 states of  $D$ -symmetry, resulting in a total dimension of the basis equal to 3470. Issues related to the convergence of the calculation with respect to the variations of the composition of the basis set are described in details in Ref. [16]. A separate calculation in which we added a subset

of 20 pseudostates with  $l = 4$  produced only a minor change (of an order of a percent) for the ionization probabilities.

Initial conditions for the solution of TDSE are determined by solving an eigenvalue problem using a subset of basis functions of the  $S$ -symmetry only. This produced the ground state energy of -2.90330 a.u. We integrate TDSE up to a time  $T_1$  when the external field is switched off. Then we project the solution onto a field-free CCC wave functions  $\Psi(\mathbf{k}_1, \mathbf{k}_2)$  representing two electrons in continuum. Details of the construction of these functions can be found, for example, in Ref. [26], or in our earlier paper [16].

A set of the final states corresponding to various photo-electron energies  $E_1, E_2$  was prepared. The energies  $E_1$  and  $E_2$  were taken on a grid  $E_i = 1, 4, 7, 10, 13, 16, 19, 22, 27, 40, 100, 200$  eV. Projection of the solution of the TDSE on the states of this grid gives us a probability distribution function  $p(\mathbf{k}_1, \mathbf{k}_2)$  of finding the helium atom in a field-free two-electron continuum state  $(\mathbf{k}_1, \mathbf{k}_2)$  at the time  $t = T_1$ .

From this probability, we can compute various differential and the total integrated cross-sections of TPDI. The fully resolved, with respect to the photoelectron angles and their energy, triply differential cross-section (TDCS) is defined as

$$\frac{d\sigma(\omega)}{dE_1 d\Omega_1 d\Omega_2} = \frac{C}{W q_1 q_2 \cos^2 \alpha} \int p(\mathbf{k}_1, k_1 \tan(\alpha) \hat{\mathbf{k}}_2) k_1 dk_1, \quad (9)$$

The total integrated cross-section (TICS) is computed as

$$\sigma(\omega) = \frac{C}{W} \int p(\mathbf{k}_1, \mathbf{k}_2) d\mathbf{k}_1 d\mathbf{k}_2 dk_1 dk_2, \quad (10)$$

Here  $W = \int_0^{T_1} F_{ac}^4(t) dt$ , and  $C = 12\pi^2 a_0^4 \tau \omega^2 c^{-2}$  is the TPDI constant expressed in terms of the speed of light in atomic units  $c \approx 137$ , the Bohr radius  $a_0 = 0.529 \times 10^{-8}$  cm and the atomic unit of time  $\tau = 2.418 \times 10^{-17}$  s. Momenta  $q_1, q_2$  in Eq. (9) are defined on the energy shell:  $E_1 = q_1^2/2$ ,  $E - E_1 = q_2^2/2$ ,  $\tan \alpha = q_2/q_1$ ,  $E$  is the excess energy.

### III. RESULTS.

There are two TPDI channels with electrons escaping into the  $S$  and  $D$  continua. In the present paper, we are able to report only results for the  $D$ -channel as we do not reach

satisfactory accuracy for the  $S$ -channel. The reason for this lies in the fact that the final state CCC wave functions in the  $S$ -channel are not completely orthogonal to the ground state wave function. These two sets of wave functions are obtained using two completely unrelated procedures. The initial ground  $^1S$  state may have, therefore, a nonzero overlap with the final state CCC wave function which, after propagation in time, may affect the  $S$ -channel TPDI results. Since the  $S$ -channel contribution to TPDI is generally a small number, this initial non-zero overlap can produce considerable inaccuracy in the calculation of the  $S$ -wave ionization.

Present results for ionization into the  $D$ -channel can be utilized in a two-fold manner. We can either consider them as the exact results for TPDI in a circular polarized ac field. In this case, only the  $D$ -wave contributes as the  $S$ -wave cannot accommodate two units of angular momentum projection acquired after absorbing two circularly polarized photons. Alternatively, we can rely on the fact that the  $S$ -wave contribution to TPDI is generally small. Thus, with some caution, we can apply the present results to linearly polarized ac field as well. To check the accuracy of our method for the  $D$ -wave, we have in our disposal the wealth of literature results for the region of photon energies from 42 to 47 eV, which has been thoroughly studied.

### A. Total integrated cross-section

Before presenting our numerical TICS results across the studied photon energy range, we wish to outline the procedure we use to attest the accuracy of our calculation. Consider the time-evolution of the helium atom in the absence of the ac external field. This evolution can be presented as a sum

$$\Psi(t) = \sum c_k \exp^{-iE_k t} \Psi_k, \quad (11)$$

where  $\Psi_k$  and  $E_k$  are solutions of the eigenvalue problem for the field-free helium Hamiltonian on the basis (7). The eigenvectors  $\Psi_k$  are not strictly orthogonal to the CCC field-free states. The overlap of the solution of the TDSE and the CCC state will therefore contain terms  $\sum c_k \exp^{-iE_k t} \langle \Psi_{\text{CCC}} | \Psi_k \rangle$ . These terms introduce beats in the computed probabilities which may affect the accuracy of the calculation considerably unless the overlaps  $\langle \Psi_{\text{CCC}} | \Psi_k \rangle$  peak

in a narrow range of energies  $E_k$ . The magnitude of these beats may serve as an indicator of the accuracy of the calculation.

This point is illustrated in Figure 1 where we plot the squared overlaps  $|\langle \Psi_{\text{CCC}} | \Psi_k \rangle|^2$  between various  $D$ -symmetry eigenfunctions of the eigenvalue problem for the field-free helium Hamiltonian on the basis (7) and a final state CCC wave function at the excess energy of 20 eV above the double ionization threshold. We see that indeed there are only few leading overlaps which peak narrowly around this energy and other overlaps are insignificant on this scale.

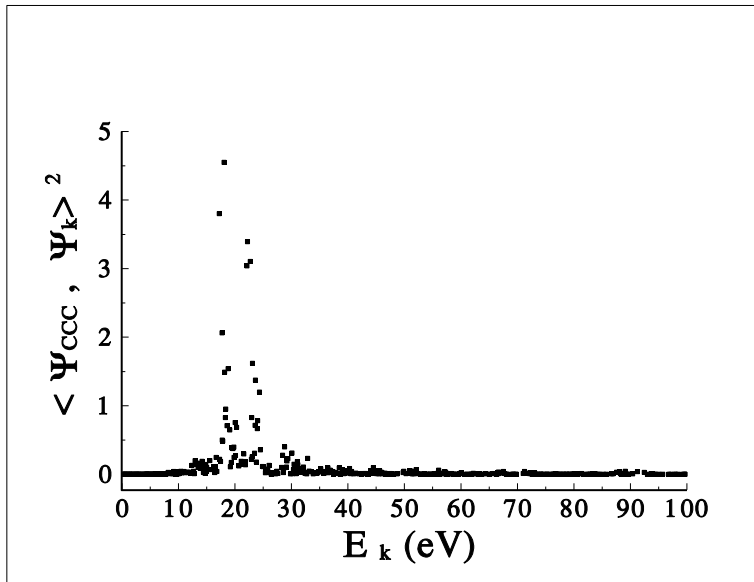


FIG. 1: Squared overlaps  $|\langle \Psi_{\text{CCC}} | \Psi_k \rangle|^2$  between various  $D$ -symmetry eigenfunctions of the eigenvalue problem for the field-free helium Hamiltonian on the basis (7) and a CCC wave function at the excess energy of 20 eV above the double ionization threshold.

Narrow localization of the overlaps on the energy scale dampens the beats considerably. This is illustrated in the Table I where we present three sets of TICS computed for several selected photon energies. These sets are obtained as follows. The first set of TICS (second column) is computed by overlapping the solution of the TDSE and the CCC wave functions at the time  $T_2 = T_1 = 6T$  when the ac field is switched off. To obtain the second set of data (third column), we let the atom evolve freely for one period after the ac field is switched off and then the overlaps with the CCC field free states are computed at the moment  $T_2 = 7T$ .

The last set of TICS (the fourth column) is obtained when the system evolves freely for two periods of the ac field after it is switched off and the overlaps are computed at the moment  $T_2 = 8T$ . As one can see from these data, the beats mentioned above lead to variations of TICS of the order of 20 percent for the photon energy range covered in the Table. We can adopt this figure as an estimate of the accuracy of the present calculation.

TABLE I: TICS (in units of  $10^{-52}$  cm<sup>4</sup>s) obtained for values of  $T_2 = 6T$ ,  $7T$ , and  $8T$ .

$\omega$	$6T$	$7T$	$8T$
42	0.500	0.443	0.506
45	0.962	0.775	0.959
48	1.459	1.298	1.374
50	1.646	1.768	1.629

For energies outside this range, results are fluctuating much more and, hence, are considerably less accurate. This can probably be explained if we recall the observation we made above about the nature of the beats in the computed probabilities. Their magnitude is determined eventually by the spectrum of the eigenvalue problem for the field-free helium Hamiltonian in the basis (7) and the set of CCC final state wave functions we use. Proceeding further into a domain of larger frequencies probably requires additional tuning of both sets.

In Figure 1, we present our results for TICS in the whole photon energy range from 42 to 50 eV studied in the paper. The “error bars” attached to our data indicate the fluctuation of TICS due to free propagation beats. In Figure 1, we compare the present calculation with known literature values obtained by the following methods: TDCC [3, 13], R-matrix [6] and TD-basis [8]. Within the stated accuracy of 20%, our results agree with the R-matrix and TD-basis calculations. The TDCC calculations of Refs. [3] and [13] differ between each other because two different shapes of the field pulse are utilized in these works: a constant amplitude pulse which is ramped on and off smoothly over one field period and a sine squared envelope, respectively. In the present calculation we employed a constant amplitude pulse and therefore our results should be compared with Ref. [3] which reported the TICS of



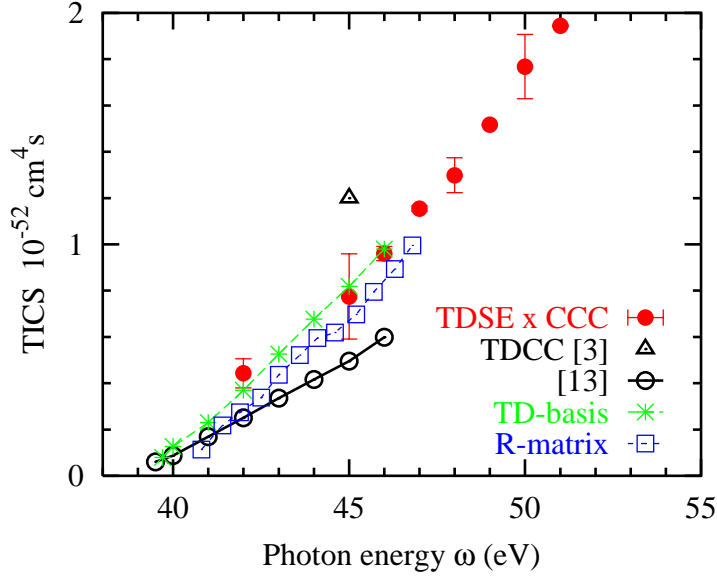


FIG. 2: Total integrated cross-section of TPDI on He as a function of the photon energy. Present results obtained by combination of the TDSE and CCC methods and corresponding to the field intensity of  $3.5 \times 10^{14}$  W/cm<sup>2</sup> are shown by red filled circles. Other calculations are as follows: TDCC with a  $\sin^2$  envelope,  $5 \times 10^{14}$  W/cm<sup>2</sup> [13], open circles; TDCC with a ramped pulse,  $10^{14}$  W/cm<sup>2</sup> [3], open triangle; TD basis,  $10^{14}$  W/cm<sup>2</sup> [8], green asterisks; R-matrix,  $10^{13}$  W/cm<sup>2</sup> [6], blue open squares.

$1.2 \times 10^{-52}$  cm<sup>4</sup>s at 45 eV of photon energy. This is quite close with our result of  $9 \times 10^{-53}$  cm<sup>4</sup>s which should further increase when the  $S$ -wave is accounted for.

### B. Fully differential cross-section

In Figure 3, we present our results for the fully resolved TDCS of TPDI of He at the photon energy of 42 eV and the equal energy sharing between two photoelectrons  $E_1 = E_2 = 2.5$  eV. We adopt the coplanar geometry in which the momenta of the two photoelectrons and the polarization vector of light belong to the same plane which is perpendicular to the propagation direction of the photon. We compare the present TDSE results with our earlier CCC calculation in the closure approximation [28]. We also present in the figure the TDCC results of Hu et al. [13] who gave in their work separate contributions of the  $D$  and  $S$ -waves to TDCS. To make a shape comparison, we divide the present calculation by the same factor

of 1.3 for all fixed electron angles. This factor reflects the difference in TICS between the two methods. We remind the reader that the TDCC calculation of Hu et al. [13] is performed with a sine squared envelope and their TICS are smaller than the present TDSE calculation. There is a fair shape agreement between the three sets of calculations except for  $\theta_1 = 60^\circ$  where the relative intensity of two major peaks is reversed between TDSE and TDCC. The CCC calculation in the closure approximation is somewhat in between the two other results.

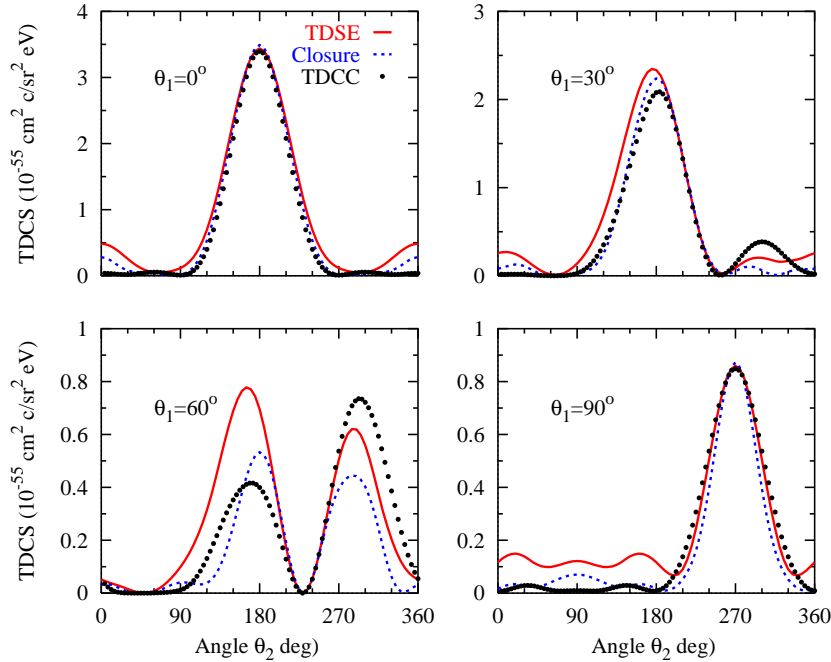


FIG. 3: TDCS of He TPDI for the coplanar geometry at  $\omega = 42$  eV and  $E_1 = E_2 = 2.5$  eV ( $D$ -wave contribution only). The present TDSE calculation (divided by 1.3) is shown by the red solid line. The earlier CCC calculation in the closure approximation (divided by 1.7) is shown by the blue dashed line. The black dots represent the TDCC results of Ref. [13].

#### IV. CONCLUSION.

In the present work, we studied two-photon double electron ionization of helium in the range of photon energies from 42 to 50 eV. The domain of energies from 42 to 47 eV has been studied extensively before and there is an abundance of theoretical results in the literature

both for the total and, to lesser extent, differential cross-sections. Our present calculations, both for TICS and TDCS, agree reasonably well with these results. Our TICS values lie on the higher end of the set of data presented in Figure 2. As we noted above, this may be, at least partially, explained by the particular pulse shape adopted in the present work. More interesting, perhaps, is the monotonous growth of TICS with the photon energy which we established for energies below 50 eV. Most probably, this feature will be present for any pulse shape. We may expect some unusual features to appear in TICS for photon energies approaching the threshold of sequential TPDI at 54.5 eV. It was shown in Refs. [17, 29] that the spectrum of emitted electrons undergoes qualitative reconstruction when the new mechanism opens up. This reconstruction may leave its trace in some additional feature of TICS. We are going to explore this new regime in the future. We also intend to resolve the issue of orthogonality and to evaluate the  $S$ -wave contribution to TPDI.

The presently analyzed fully differential cross-sections (TDCS) agree very well between the two CCC calculations: the non-perturbative TDSE and the perturbative closure. In these two models, we employ the same CCC final state whereas theoretical description of the field interaction with the atom is different. The fact that the differential cross-sections are similar in these two calculations indicates that the energy and angular correlation in the two-electron continuum is established as the result of the electron correlation in the final doubly ionized state. It shows little sensitivity to the precise mechanism of the atom-field interaction.

## V. ACKNOWLEDGEMENTS

We wish to thank James Colgan for supplying the data in numerical form. The authors acknowledge support of the Australian Research Council in the form of the Discovery grant DP0451211. Facilities of the Australian Partnership for Advanced Computing (APAC) were used.

---

[1] M. Protopapas, C. H. Keitel, and P. L. Knight, Rep. Prog. Phys. **60**, 389 (1997).

- [2] A. Becker, R. Dörner, and R. Moshhammer, *J. Phys. B* **38**, S753 (2005)
- [3] J. Colgan and M. S. Pindzola, *Phys. Rev. Lett.* **88**, 173002 (2002).
- [4] T. Mercouris and C. A. Nicolaides, *J. Phys. B* **21**, L285 (1989).
- [5] C. A. Nicolaides and T. Mercouris, *Chem. Phys. Lett.* **159**, 45 (1989).
- [6] L. Feng and H. W. van der Hart, *J. Phys. B* **36**, L1 (2003).
- [7] G. L. Kamta and A. F. Starace, *Phys. Rev. A* **65**, 053418 (2002).
- [8] B. Piraux, J. Bauer, S. Laulan, and H. Bachau, *Eur. Phys. J. D.* **26**, 7 (2003).
- [9] P. Lambropoulos, P. Maragakis, and J. Zhang, *Phys. Rep.* **305**, 203 (1999).
- [10] A. Scrinzi and B. Piraux, *Phys. Rev. A* **58**, 1310 (1998).
- [11] J. Caillat, J. Zanghellini, M. Kitzler, O. Koch, W. Kreuzer, and A. Scrinzi, *Phys. Rev. A* **71**, 012712 (2005).
- [12] M. S. Pindzola and F. Robicheaux, *J. Phys. B* **31**, L823 (1998).
- [13] S. X. Hu, J. Colgan, and L. A. Collins, *J. Phys. B* **38**, L35 (2005).
- [14] J. Colgan and M. S. Pindzola, *J. Phys. B* **37**, 1153 (2004).
- [15] T. Mercouris, C. Haritos, and C. A. Nicolaides, *J. Phys. B* **34**, 3789 (2001).
- [16] I. A. Ivanov and A. S. Kheifets, *Phys. Rev. A* **74**, 042710 (2006).
- [17] S. Laulan and H. Bachau, *Phys. Rev. A* **68**, 013409 (2003).
- [18] A. Becker and F. H. M. Faisal, *J. Phys. B* **38**, R1 (2005).
- [19] C. W. McCurdy, T. N. Rescigno, and D. Byrum, *Phys. Rev. A* **56**, 1958 (1997).
- [20] M. Baertschy, T. N. Rescigno, and C. W. McCurdy, *Phys. Rev. A* **64**, 022709 (2001).
- [21] C. W. McCurdy, D. A. Horner, T. N. Rescigno, and F. Martin, *Phys. Rev. A* **69**, 032707 (2004).
- [22] M. Pont and R. Shakeshaft, *Phys. Rev. A* **51**, 494 (1995).
- [23] L. Malegat, P. Selles, and A. K. Kazansky, *Phys. Rev. Lett.* **85**, 4450 (2000).
- [24] J. Colgan and M. S. Pindzola, *Phys. Rev. Lett.* **88**, 173002 (2002).
- [25] I. Bray, *Phys. Rev. A* **49**, 1066 (1994).
- [26] I. Bray and A. T. Stelbovics, *Adv. Atom. Mol. Phys.* **35**, 209 (1995).
- [27] D. V. Fursa and I. Bray, *J. Phys. B* **30**, 757 (1997).
- [28] A. S. Kheifets and I. A. Ivanov, *J. Phys. B* **38**, 471 (2006).
- [29] S. Laulan, H. Bachau, B. Piraux, J. Bauer, and G. L. Kamta, *Journal of Modern Optics* **50**, 353 (2003).